Equatorial Scintillation Predictions from C/NOFS Planar Langmuir Probe Electron Density Fluctuation Data

Emanoel Costa[1], Patrick Roddy[2], Kyle Wiens[2], and Cesar Valladares[3]

[1]Centro de Estudos de Telecomunicações, Pontifícia Universidade Católica do Rio de Janeiro, Rua Marquês de São Vicente 225, 22451-900 Rio de Janeiro RJ Brazil, e-mail: epoc@cetuc.puc-rio.br

[2]Space Vehicles Directorate, Air Force Research Laboratory, Kirtland Air Force Base, NM, U.S.A., e-mails: patrick.roddy@us.af.mil, kyle.wiens.1@us.af.mil

[3]Institute for Scientific Research, Boston College, Chestnut Hill, MA, U.S.A., e-mail:cesar.valladares@bc.edu

This paper was prepared for presentation during the 14th International Congress of the Brazilian Geophysical Society held in Rio de Janeiro, Brazil, August 3-6, 2015.

Abstract: The present contribution will apply a phase-screen and weak-scattering scintillation algorithms to *in situ* data from the Planar Langmuir Probe onboard the Communication/Navigation Outage Forecasting System satellite to predict value of the scintillation index S_4. The results from the models will be compared with measurements performed by the 244-MHz SCINDA receivers located at Ancon, Peru (11.8°S, 77.2°W).

Introduction

Ionospheric scintillation exhibits extreme variability in space and time, significantly degrading both the performance and the availability of space-based communication and navigation systems. For the support of these systems at equatorial and low latitudes, short-term scintillation forecast systems based on real-time measurements explore the facts that the irregularities are field-aligned, their motion is ordered, and their lifetime is relatively long [1]. One such supporting system, the Communication/Navigation Outage Forecasting System (C/NOFS) [2] is based on a non-geostationary equatorial satellite successfully launched in an elliptical orbit with 400-km perigee, 850-km apogee and orbital inclination of 13° on April 16, 2008. Due to its orbital period, the satellite is able to track the evolution and motion of plasma bubbles at 90-min intervals. Data from sensors on board the satellite drive an equatorial ionospheric model to forecast the onset of plasma instability and its evolution (plasma bubbles). A phase screen model is used to determine the magnitude of phase and intensity scintillation of satellite signals propagating through the turbulent medium and received on the ground. These calculations are validated by scintillation measurements performed using beacon transmissions.

Recent work [3] on the development and application of a radio wave scattering algorithm to predict scintillation due to the slant propagation through an irregularity medium characterized by combined data from the São Luís coherent scatter radar (2.57° S, 44.21° W, dip angle 1.73°) and the C/NOFS Planar Langmuir Probe (PLP). Although the results seem promising, the developed algorithms should be: (1) adapted to rely only on space-based data; (2) more extensively tested; and (3) extended to other locations and frequencies of interest. This is the main objective of the present contribution: a phase-screen and weak-scattering scintillation algorithms will be applied to *in situ* C/NOFS PLP data to predict value of the scintillation index S_4. The results from the models will be compared with measurements performed by the 244-MHz SCINDA receivers located at Ancon, Peru (11.8°S, 77.2°W).

Description of Scintillation Models and Data

The present model assumes that, due to the fast velocity (approximately 7.5 km/s) of the C/NOFS satellite, the PLP data provides a near-instantaneous and high-resolution snapshot of the irregularity structures that drift along the geomagnetic west-to-east direction with a relatively slow velocity, typically in the range from 80 m/s to 150 m/s. It uses a properly scaled version of electron density fluctuations directly measured by the PLP on board the C/NOFS satellite. This model could be combined with a mapping of the measured electron density fluctuations along field lines defined by the International Geomagnetic Reference Field (IGRF-11), to create an extended phase screen that drifts over selected ground stations during long periods of time according to a measured or climatological local-time pattern. However, for the present application, the scintillation calculations assume horizontal geomagnetic field lines and an irregularity layer with fixed thickness and drift velocities for the phase screen which are consistent with climatological models. At equally-spaced and short time intervals, the position of the phase screen with respect to the ray paths from geostationary satellite to the receiver is updated. The spaced-based scintillation model is then applied to the local phase screen centered at each ray path to estimate the corresponding scintillation index S_4. The basic features of the model are sketched in Figure 1.

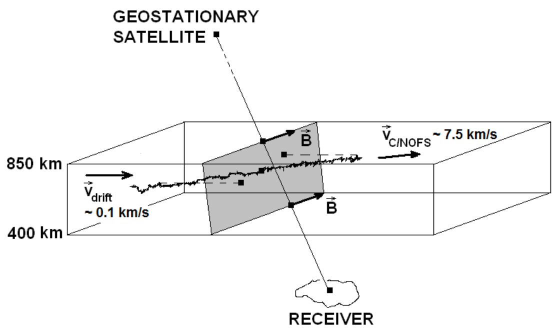

Figure1. Basic features of the spaced-based scintillation model.

The results from the model will be compared with those from another model based on the weak-scattering theory [4-7], which estimates the scintillation index S_4 from several irregularity layer parameters using the equation

$$S_4 = C(sec\psi)\left(r_e\lambda\sqrt{LL_o}\right)\Delta N\left(\sqrt{2\pi\lambda z}/L_o\right) \qquad (1)$$

In the above equation, ψ is the zenith angle of the ray path, r_e = 2.8179 x 10^{-15} m is the classical electron radius, λ is the wavelength, L and z are the irregularity layer thickness and bottom height, respectively, ΔN is the rms electron density fluctuations, and L_o is the outer scale size of their power spectral density. Depending on the power spectral density model of the ionospheric irregularities assumed by different authors [4-7], the parameter C may vary from approximately 0.6 to 2.0. Calculation results will also be compared with measurements performed by the 244-MHz SCINDA receivers located at Ancon, Peru (11.8^{o}S, 77.2^{o}W). The projections of the ray paths onto the Google Earth map of the relevant part of South America are shown in Figure 2.

Figure 2. Projections of the Ancon 250-MHz SCINDA ray paths onto the Google Earth map of South America.

The SCINDA scintillation and drift velocity data are available in individual daily files (from 43200 UT in one day to 43200 UT in the following day) with approximately 65-s (roughly 1-min) resolution. Each 1-min record associates the date (YY/DDD) and Universal Time (s) to: (1) the corresponding S_4 values for five fixed links (four operating at 244 MHz and one at 1500 MHz); and (2) drift velocities. Both Ancon 244-MHz SCINDA links are affected by scintillation. Indeed, Figure 3 shows, for each evening of the year 2009 (solar minimum), the number of minutes with S_4> 0.4 and S_4> 0.7 for the West (blue) and East (red) links. The green curve also shows the number of evening minutes available for at least one of the links. It is observed that the scintillation index S_4 may exceed 0.4 for several hours during a single evening on both links.

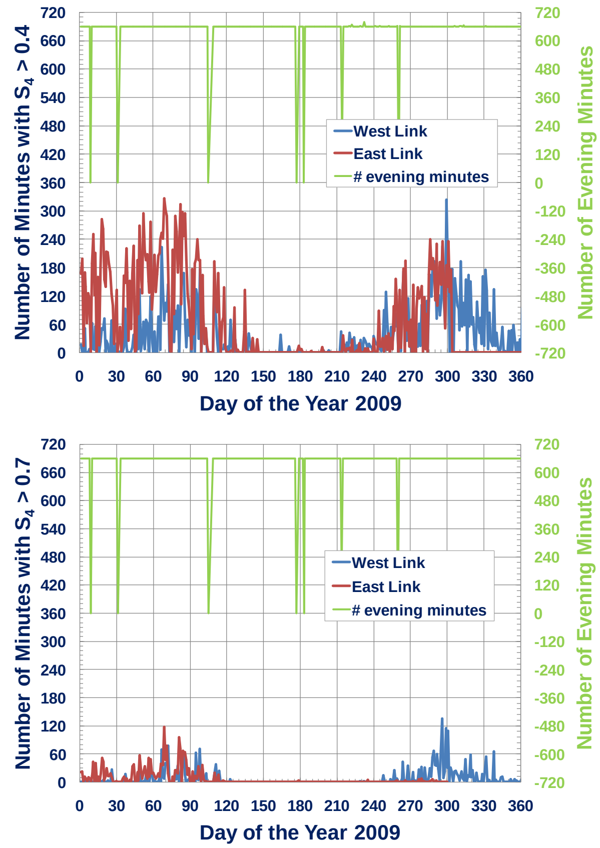

Figure 3. Number of minutes with S_4 > 0.3 in the West (blue) and East (red) links and number of evening minutes available for at least one of the links (green). Note that only West link data are available from day 300 of the year 2009 (solar minimum).

It should be remarked that the minutes with scintillation activity displayed in Figure 3 are not necessarily contiguous. Figure 4 shows the distribution of the duration (minutes) of scintillation events with S_4 > 0.4 (upper plot) and S_4 > 0.7 (lower plot). Figure 5 shows the distribution of the duration (minutes) of intervals between consecutive scintillation events (interevents) with S_4 > 0.4 (upper plot) and S_4 > 0.7 (lower plot). It is seen that most of the scintillation events are relatively short and also spaced by short intervals.

Results from a Weak-Scattering Scintillation Model

It is assumed that irregularities drift across the horizontal magnetic field line, as represented by the dashed lines in Figure 1. Using the associated information on Universal Time and position (latitude, longitude and altitude) in combination with the fixed drift velocity, the position (represented by the black square dots in Figure 1) and the local time at which the sample would reach the gray plane defined by the ray path and the geomagnetic field have been obtained.

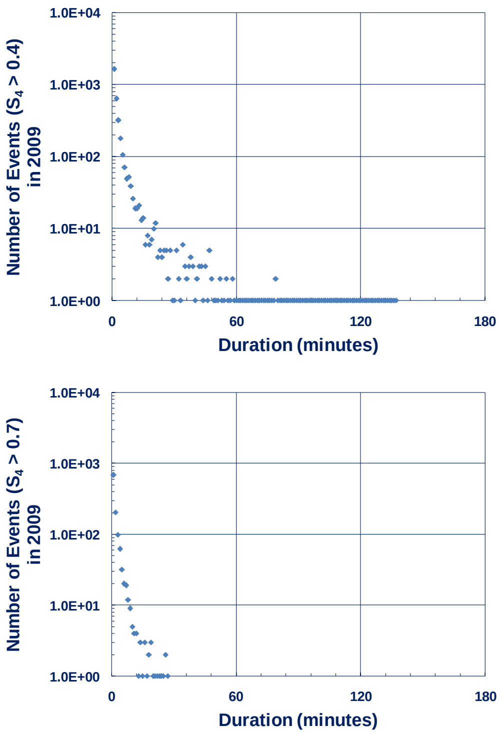

Figure 4. Distribution of the duration (minutes) of scintillation events with $S_4 > 0.4$ (upper plot) and $S_4 > 0.7$ (lower plot) during 2009 (solar minimum).

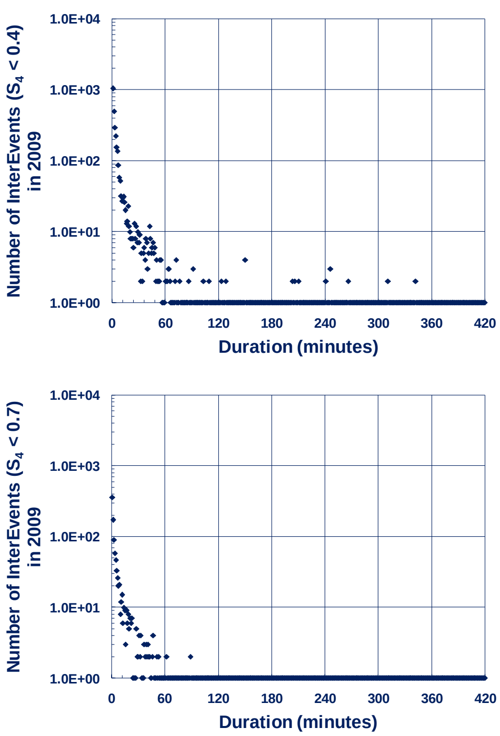

Figure 5. Distribution of the duration (minutes) of scintillation interevents with $S_4 > 0.4$ (upper plot) and $S_4 > 0.7$ (lower plot) during 2009 (solar minimum).

Assuming field-aligned irregularities, this sample would have affected propagation along the VHF SCINDA West link at the determined local time. Next, a weak-scattering scintillation model has been applied to each *in situ* PLP data sample corresponding to sections of C/NOFS orbits observed from Ancon with high elevations. Fixed values for the irregularity drift velocity (v_D = 100 m/s), outer scale size (L_o = 12.5 km), spectral index n = 1.7, layer thickness (L = 100 km) and height (z = 400 km) have been assumed. Combining these values with that from each measured sample of the rms electron density fluctuation ΔN, the corresponding value of S_4 has been determined using equation (1). Additionally, these parameter values have also been applied to simulate samples of received signals using a numerical model based on a parabolic approximation of the wave equation [8]. Then, the associated value of S_4 has been calculated from the sample of the received signal. Finally, the obtained S_4 time series have been smoothed by the application of a 30-minute running mean, Results from the second of these S_4 calculations for the VHF SCINDA West link are represented by the red curves in Figure 6 for the days 06-07 April 2009 (upper plot) and 20-21 December 2009 (lower plot), for the periods of available C/NOFS PLP data. Direct and continuous measurements of S_4 due to propagation along the same link are represented by the blue curves in the same Figure. Note that the system imposes the approximate floor $S_4 > 0.15$ to measurements, which is not present in the calculations.

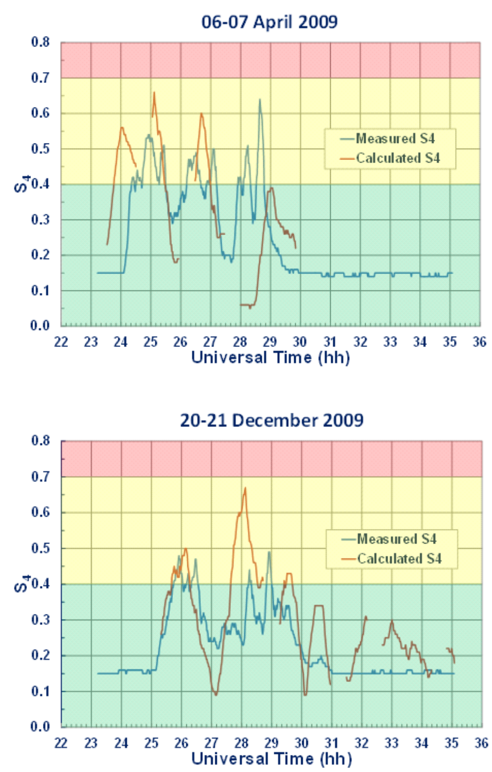

Figure 6. (Red) S_4 calculations for the VHF SCINDA West link for the days 06-07 April 2009 (upper plot) and 20-21 December 2009 (lower plot), for the periods of available C/NOFS PLP data. (Blue) Direct and continuous measurements of S_4 due to propagation along the same link.

Figure 7 shows the distribution of errors S_{4meas}-S_{4calc} between measurements and calculations for the year 2009, considering 67146 error samples resulting from measurements and calculations associated with the same local time. The distribution is highly peaked, with a bias of 0.1.

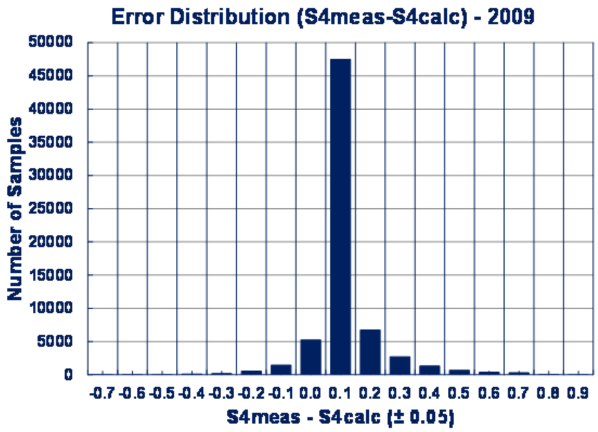

Figure 7. Distribution of errors S_{4meas}-S_{4calc} between measurements and calculations for the year 2009.

Conclusion

Scintillation calculations based only on *in situ* C/NOFS PLP data have been extensively compared with S_4 measurements from the SCINDA VHF West link at Ancon, Peru, to assess the prediction capability of the model, as well as its limitations. It should be remarked that the model displays many sources of uncertainties: frozen-in and field-alignment assumptions, layer thickness, spectral representation of irregularities, altitude effect, drift-velocity pattern from space-based measurements, as well as propagation models themselves. The displayed prediction is generally fair, but may be critical during disturbed conditions. Critical cases are under special analysis aimed at improving the prediction capability of the model. In particular, a more precise characterization of the irregularity medium may improve the forecasting capability of the described model.

Acknowledgments

Emanoel Costa was supported by AFOSR Award FA9550-12-1-0031 during the present work.

References

1. S. Basu, K. M. Groves, Su. Basu, and P. J. Sultan, “Specification and Forecasting of Scintillations in Communication/Navigation Links: Current Status and Future Plans,” *J. Atmos. Sol. Terr. Phys.*, **64**, pp. 1745-1754, November 2002.

2. O. de La Beaujardière, and the C/NOFS Science Definition Team, “C/NOFS: a Mission to Forecast Scintillation,” *J. Atmos. Sol. Terr. Phys.*, **66**, pp. 1573-1591, November 2004.

3. E. Costa, E. R. de Paula, L. F. C. Rezende, K. M. Groves, P. A. Roddy, E. V. Dao, and M. C. Kelley, “Equatorial Scintillation Calculations Based on Coherent Scatter Radar and C/NOFS Data,” *Radio Sci.*, **46**, pp. RS2011.1-RS2011.21, April 2011.

4. C. L. Rufenach, “Ionospheric Scintillation by a Random Phase Screen: Spectral Approach,” *Radio Sci.*, **10**, pp. 155-165, February 1975.

5. Su. Basu, S. Basu, and B. K. Khan, “Model of Equatorial Scintillation from In-situ Measurements,” *Radio Sci.*, **11**, pp. 821-832, October 1976.

6. E. Costa, and M. C. Kelley, “Ionospheric Scintillation Calculations Based on In-situ Irregularity Spectra,” *Radio Sci.*, **12**, pp. 797-809, October 1977.

7. C. L. Rino, “A Power Law Phase Screen Model for Ionospheric Scintillation: 1. Weak Scatter,” *Radio Sci.*, **14**, pp. 1135–1145, December 1979.

8. E. Costa, and S. Basu, “A radio wave scattering algorithm and irregularity model for scintillation predictions,” *Radio Sci.*, 37, pp. 18.1-18.14, June 2002.